applied sciences

MDPI

Article

Stress Analysis and Structural Improvement of LNG Tank Container Frames under Impact from Railway Transport Vehicles

Zhiqiang Wang, Caifu Qian and Zhiwei Wu *

College of Mechanical and Electrical Engineering, Beijing University of Chemical Technology, Beijing 100029, China; w2020400168@163.com (Z.W.); qiancf@mail.buct.edu.cn (C.Q.)
* Correspondence: zwzhiweiwu@163.com

Abstract: As the stress of the frame, especially the bottom side rail supports and bottom inclined supports, of a traditional LNG tank container could be significantly greater than its allowable stress, and the container cannot meet the strength requirement of the specification when it is impacted by a transport vehicle during railway transportation, three improved frame structures were suggested, which removed or changed the side rails or bottom inclined supports; the stress and deformation of these improved frames and the tank container were analyzed using the finite element method under the impact test. The results show that all three improved frames can meet the strength requirement, i.e., the maximum Mises stress is less than the allowable stress and the deformation requirement of the diagonal length difference is less than the allowable value, meaning that the tank containers with improved frames can pass the impact test. Moreover, for the FRP support rings and impact side heads, although the maximum values are different, they are still less than the respective allowable stresses. In addition, the maximum value of the middle cross section of the outer vessel in the direction of gravity does not increase with the change in the frame, and the deformation of the outer vessel remains within the elastic range. Therefore, the improvements of the frames have little effect on the stress and deformation of the other components of the tank container, in particular, the inner vessel and outer vessel. Compared to the frame of the traditional tank container, removing the side rails partially or completely can reduce the weight of the frame by 17.99% and 38.34%, respectively, greatly reducing manufacturing and transportation costs. It can also reduce the maximum Mises stress by 38.89% and 39.24% and the maximum diagonal difference by 57.95% and 61.16%.

Keywords: tank container; impact test; structural improvement; numerical simulation

check for updates

Citation: Wang, Z.; Qian, C.; Wu, Z. Stress Analysis and Structural Improvement of LNG Tank Container Frames under Impact from Railway Transport Vehicles. *Appl. Sci.* **2023**, *13*, 13335. https://doi.org/10.3390/app132413335

Academic Editor: Asterios Bakolas

Received: 7 November 2023
Revised: 12 December 2023
Accepted: 14 December 2023
Published: 18 December 2023

1. Introduction

During railway transportation, the stress state of tank containers, especially the frame, will be drastically changed due to impact from transport vehicles, accompanied by high local stresses, which may lead to damage to the frame in the form of strength failure and affect the safety of tank containers. Therefore, it is essential to analyze the stress and deformation of the frame under impact to ensure that it meets the corresponding specifications. Furthermore, reducing the weight of the frame while maintaining its safety can save transportation costs, which also has a high significance in engineering applications.

Studies on tank containers have been extensively performed. Wang et al. [1] introduced a novel technique for determining the vacuum pressure of tank containers: measuring the temperature (T0) of the outside surface of the multilayer insulating material. The vacuum pressure tank containers with multilayer insulation material can be easily and consistently monitored using this technology. Yu et al. [2] used three different types of experiments—prototype, field, and self-pressurization experiments—to examine how ship motion affected the pressurization and holding time of LNG tank containers. Vrabel et al. [3] assessed the movement of semitrailer vehicles carrying tank containers during and right after forceful braking. They also conducted a comparison between tank containers that had breakwater plates and those that did not. Kim et al. [4] addressed the feasibility of using a tank container as the fuel tank for an LNG-fueled ship and investigated the advantages of doing so. Additionally, static analysis of the structure using the finite element method and the impact test was performed. Peng et al. [5] carried out a transportation test for LNG tank containers in order to evaluate the safety of LNG tank container transportation on waterways. The test findings show that the LNG tank container's pressure increased gradually throughout waterway transportation, staying within a safety range. Fomin et al. [6–8] discovered that fittings' impact interaction with corner castings causes increased stresses in both containers and the flat wagon's structural components. To decrease the impact loads, it was suggested that fittings were filled with viscous or viscoelastic compounds with dumping or anticorrosive qualities. Furthermore, because of the potential for movements of the tank container in relation to the flat wagon frame because of a technological gap in the pair "fitting stop-fitting", the acceleration exceeds that allowed by the regulatory standards. A 3D finite element model was created by Sergeichev et al. [9] to simulate the shape and real layups of the wound and infused composite layers of the tank. In addition to the normative load instances, coupled Eulerian–Lagrangian analyses were used to perform the FE simulation of the dynamic crash test. The finite element research was carried out under various design loads and operating conditions by Muttaqie et al. [10], who provided a thorough method for figuring out the scantling size of the LNG-type 20 ft ISO container. According to Liguori et al. [11], the highest value of the stresses can be significantly reduced by altering parameters like the plate and skirt thickness and then acting on the arrangement of the corner supports. This improves the distribution of stiffness in the structure and reduces the weight of the tank container, albeit slightly. Real holding time testing was conducted on ISO LNG tank containers by Ryou et al. [12]. The internal pressure of the LNG tank container immediately increased upon LNG filling, then it decreased throughout container movement, according to the results. But with time, it stabilized and began to follow the graph of liquid–vapor equilibrium. In order to determine how dynamic qualities depend on factors such as amplitude, frequency, gap size, and others, De Souza et al. [13] simulated a seven tier stack made up of a scaled model of a 20 ft ISO freight container and its linking connectors. The stack was then subjected to a dynamical stress caused by the container's base. Stress analysis and strength testing were carried out for a tank container by Wang et al. [14]. The findings demonstrate that the inertial force determines the Mises equivalent membrane stress at the frame, while at the inner vessel, it is dependent upon internal pressure, even though the inertial force can sometimes have a major impact. Furthermore, Wang et al. [15] also conducted experiments and numerical simulations to investigate the impact process of a large LNG tank container for trains. They discovered that the tank container's maximum axial acceleration can reach 63 m/s^2, which is greater than the 4g inertial acceleration specified in the container design standard. This indicates that, when evaluated by the impact, the standard's specifications are not conservative. The dynamic and static finite element modeling of the tank container for use in rail and road environments was investigated by Tiernan et al. [16]. The FEA results were used to design and build a new modular tank and frame. The tank container was subsequently examined in France in compliance with Lloyds certification standards. The fluid flow inside the new tank container was investigated by Yue et al. [17]. The maximum impact force rose as the liquid filling ratio, braking deceleration, and medium density increased, according to the results. Additionally, compared to the regular tank container, the new tank container's carrying capacity increases by 11.8%. Kim et al. [18] used impact analysis software to numerically examine the effect of a bird hit on a composite container for an exterior auxiliary fuel tank. The composite container's maximum stress, deformation, and strain were calculated. The medium filling strategy for LNG tank container impact testing was proposed by Cao et al. [19]. It involves filling the tank with water to a mass equivalent to that of the dangerous items. The two tank conditions are comparable, according to retest results, and test conditions can be used to mimic real-world filling circumstances. Lee et al. [20] carried out finite element analysis on a 40-foot ISO LNG tank under low cycle condition and high cycle condition using Ansys workbench software (Version: 18.0). The findings indicated that the 40-foot LNG ISO tank container was satisfied with a fatigue life of 20 years and that the overall number of cycles was higher than the entire number of design cycles. Ashok et al. [21] conducted a comparison analysis of the unique 2.5-dimensional (2.5D) infilled structure inspired by snowflakes and six nature-inspired geometries. They also explored the impact of supported ribs and infill configurations on the crushing behavior of the structure. The suggested lightweight 2.5D infill structures show a notable increase in MCF, specific energy absorption, and limited crushing deformation, according to the results.

Through the above review, it is found that the studies on tank containers were primarily focused on the action of internal pressure and fluid temperature variations. Few studies were concentrated on the impact process of large LNG tank containers for trains and investigated the stress and deformation of the frame during this process. In this paper, the stress and deformation of a traditional LNG tank container frame under impact from railway transport vehicles were analyzed, and three improved frames were suggested to meet the strength and deformation requirements and reduce the weight of the frames.

2. Numerical Models

2.1. Geometrical Models

The studied tank container (1AA) is composed of the inner and outer vessels, eight support rings, and a frame. Rigid cubes were used to simulate the impact and transport vehicles. Twist locks were secured to the transportation vehicle. The front and rear ends of the tank are not structurally identical, so impact tests are required on both ends. Figure 1 shows the geometric models where the rear ends of the tanks were impacted. Among them, Figure 1a is the traditional frame while Figure 1(b.1–d) are three suggested improved frames. For improved frame b, the angle between the bottom side rail and its support was changed and the bottom inclined supports were removed. For improved frame c, the angle and connection location between the bottom inclined support and the corner fitting were altered and the bottom side rails were removed. For improved frame d, the top side rails in the improved frame c were removed. Compared to the traditional frame, the weight of frame c and frame d is reduced by 17.99% and 38.34%, respectively. Table 1 lists the main parameters of the tank containers.

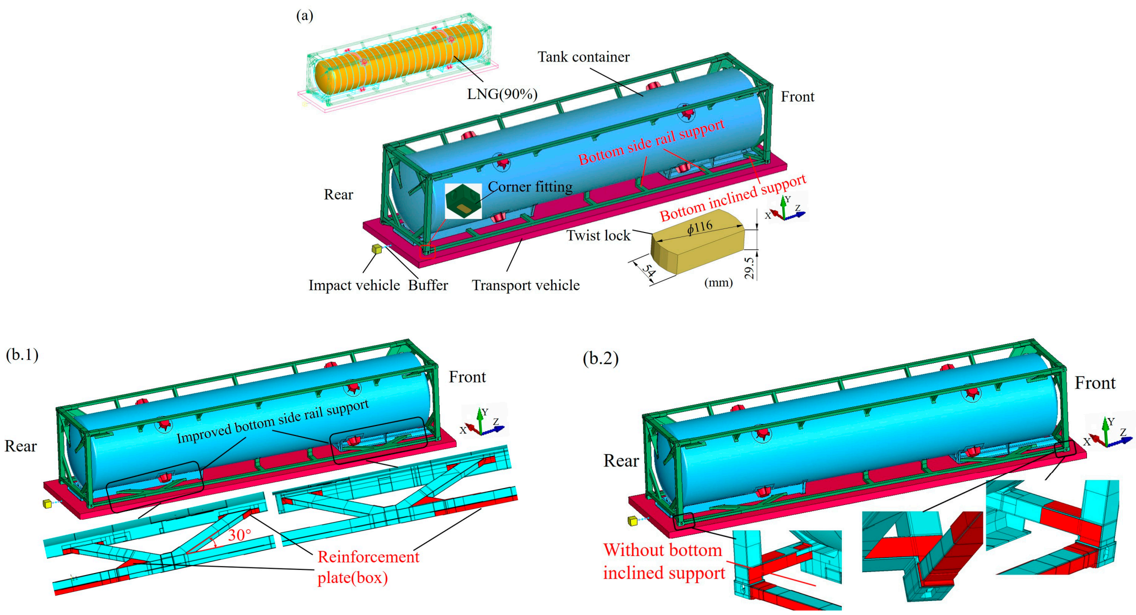

Figure 1. *Cont.*

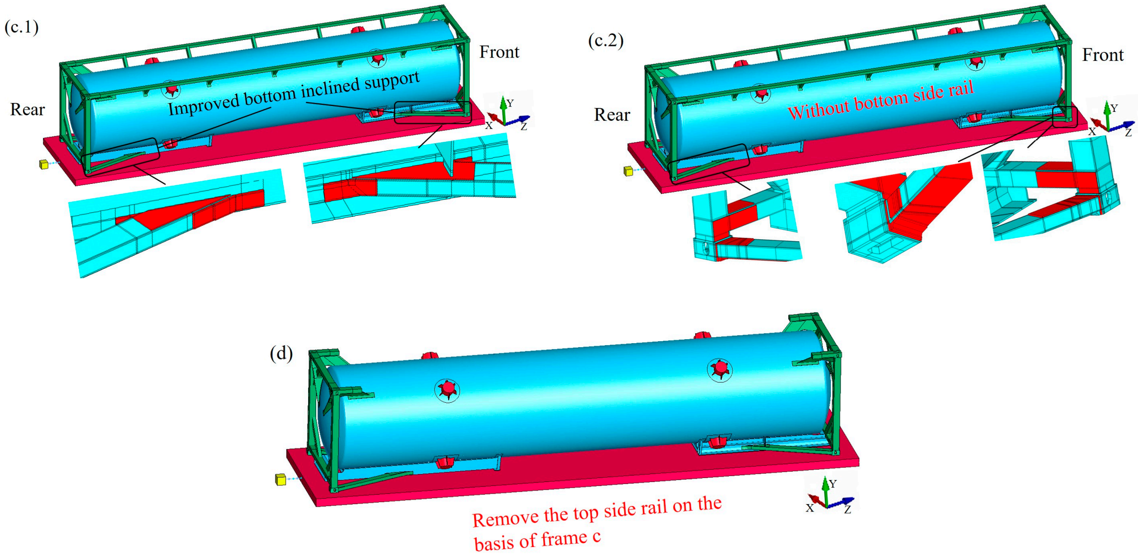

Figure 1. Geometrical models of tank containers. (**a**) Traditional frame, (**b.1**,**b.2**) improved frame b, (**c.1**,**c.2**) improved frame c, (**d**) improved frame d.

Table 1. Main design parameters of the tank container.

Item	Value	Item	Value
Specified filling rate	90%	Material of the 8 support rings	GFRP
Design pressure of the inner vessel	0.6 MPa	Material of the frame	Q450NQR1 [22]
Design temperature of the inner vessel	−196 °C	Material of the outer vessel	16MnDR [23]
Design pressure of the jacket	−0.1 MPa	Material of the inner vessel	S30408 [24]
Design temperature of the jacket	50 °C	Corrosion allowance	0

2.2. Mesh Model

The fluid is described using the ALE algorithm, the tank container is described using the Lagrangian algorithm, and the connection between the two is accomplished using the penalty function method. A spring element was used to simulate the buffer, and the initial location of the LNG in the tank container is determined using the volume fraction initialization method. The simulations in this paper were performed based on the MPP version of the dynamic software LS-DYNA (Version: R8.1.0). Figure 2 shows the mesh model of the traditional structure.

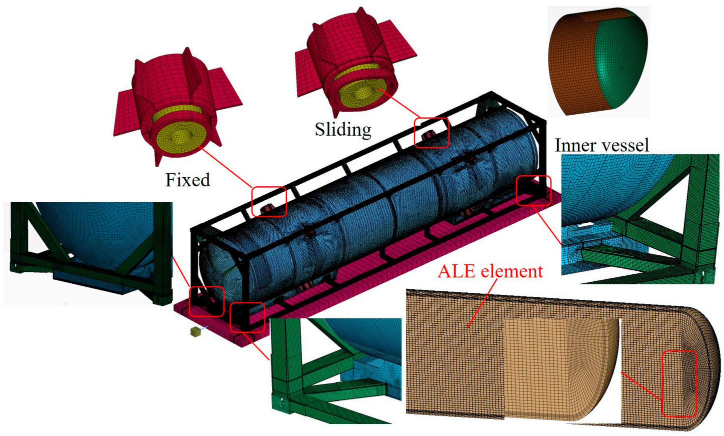

Figure 2. Mesh model of the traditional tank container.

2.3. Load and Boundary Conditions

In addition to the LNG and tank container weight, the load also consists of the internal and outer pressures (both 0.1 MPa). The following boundaries were set. (1) The impact and transport vehicle simply moved along the rail and the movement in other directions was constrained. (2) Friction contact was employed between the corner fittings and the transport vehicle, between the support rings and the vessel, and between the corner fittings and twist locks. Only the two bottom corner fittings at the impact end are impacted by the twist locks. (3) The zero is the instantaneous moment of collision between the impact vehicle and the transport vehicle. The initial velocity of the impact vehicle was 8 km/h and there was an initial clearance of 8 mm in the impact direction between the corner fittings and twist locks.

2.4. Material Models

The true stress–strain curves for the Q450NQR1, 16MnDR, and S30408 materials were used [15]. Table 2 lists other structural material properties. The material properties of LNG are listed in Table 3, with data obtained from Refprop (Version: 9.0), a specialized software for cryogenic physical properties. Using the experimental data, the force–displacement curve was generated to simulate the buffer's mechanical performance [25].

Table 2. Other structural material properties.

Item	Density (t/mm^3)	Elastic Modulus (MPa)	Poisson's Ratio
Impact vehicle	0.115×10^{-4}	0.201×10^{6}	0.3
Transport vehicle	0.295×10^{-8}	0.201×10^{6}	0.3
Twist lock	0.785×10^{-8}	0.201×10^{6}	0.3
Corner fitting	0.785×10^{-8}	0.201×10^{6}	0.3
GFRP	0.185×10^{-8}	0.720×10^{5}	0.26

Table 3. Material properties of LNG.

Item	Value	Item	Value
Temperature (°C)	−161.87	c_V (J/kg·k)	2056.3
Pressure (MPa)	0.1	k_T (1/Pa)	2.22×10^{-9}
Density (kg/m^3)	460	α (1/K)	0.00346
Sound velocity (m/s)	1341.3	γ_0	1.648
Viscosity (MPa·s)	0.118×10^{-9}		

2.5. Model Verification

The independence of load steps and meshes, as well as the reasonableness of fluid–solid coupling contact parameters, has been confirmed with an error of only 2.13%. To verify the rationality of the model, the impact strength test was carried out according to the Chinese standard *TB/T1335-1996* [26]. The impact vehicle collided with a stationary, non-braking transport vehicle equipped with the test tank container at specific velocities of 4 km/h, 5 km/h, 6 km/h, 7 km/h, and 8 km/h. After the collision between the impact vehicle and the transport vehicle, the twist lock attached to the transport vehicle collided with the corner fittings of the tank container. The two vehicles were then connected by buffers and traveled together in the direction of the rail. In order to measure stress, several strain gauges were installed on the tank containers, especially on the frame. The results indicate that the simulation results are in good agreement with the experimental results, suggesting that the finite element model is reasonable [15].

3. Results and Discussion

The force direction involved in the section is along the rail direction, i.e., the impact direction. The positive and negative directions of the force are consistent with the positive and negative directions of the *Z*-axis in Figure 1.

3.1. Frame Mises Stress Analysis

Figure 3 shows the stress distribution in the traditional frame at the moment of the first stress peak and the variation in stress at some locations over time when only the rear end or front end of the tank container was impacted. Corner fittings are standard parts, so they are not considered in the stress analysis. According to the Chinese standard *TB/T 1335-1996* [26], the maximum Mises stress of the frame should be less than the allowable stress (Q450NQR1,382MPa as shown by straight line in Figures 3–6). It is evident that the stress at many locations on the bottom side rail supports and bottom inclined supports far exceeds the allowable stress at many moments, and improvements to the frames are needed.

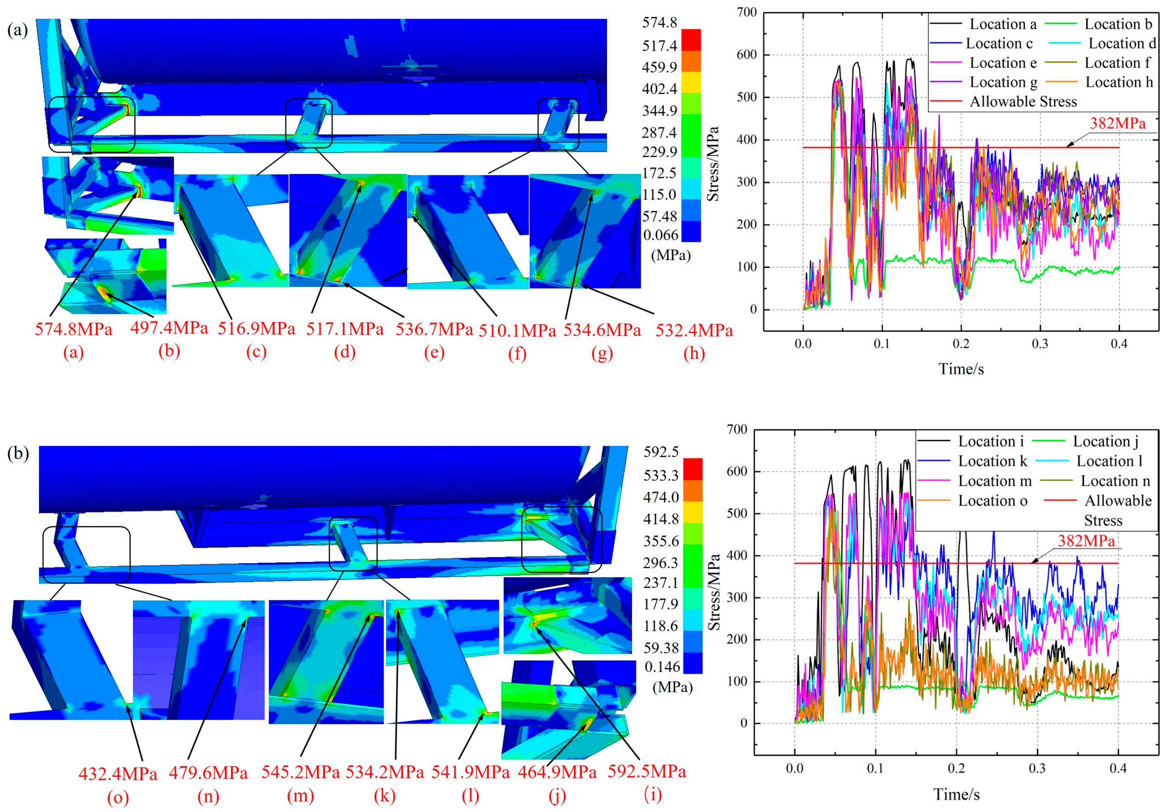

Figure 3. The stress distribution of the traditional frame and the variation in stress over time: (**a**) only the rear end was impacted; (**b**) only the front end was impacted.

By adjusting the support angle and applying reinforcement plates, the maximum Mises stresses of the three improved frames are less than 382 MPa throughout the entire simulation process, meeting the strength requirement. Figures 4–6 show the stress distribution in frame b to frame d at the moment of the first stress peak and the variation in stress at some locations over time when only the rear end or front end of the tank container was impacted.

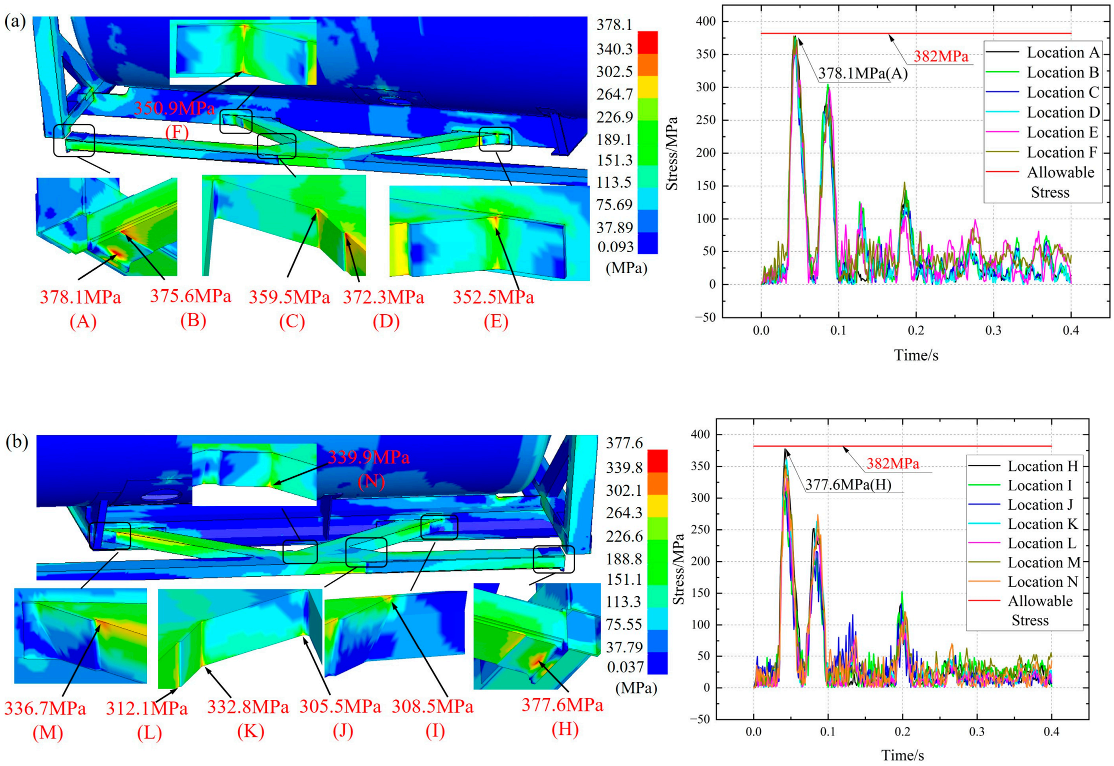

Figure 4. The stress distribution of the frame b and the variation in stress over time: (**a**) only the rear end was impacted; (**b**) only the front end was impacted.

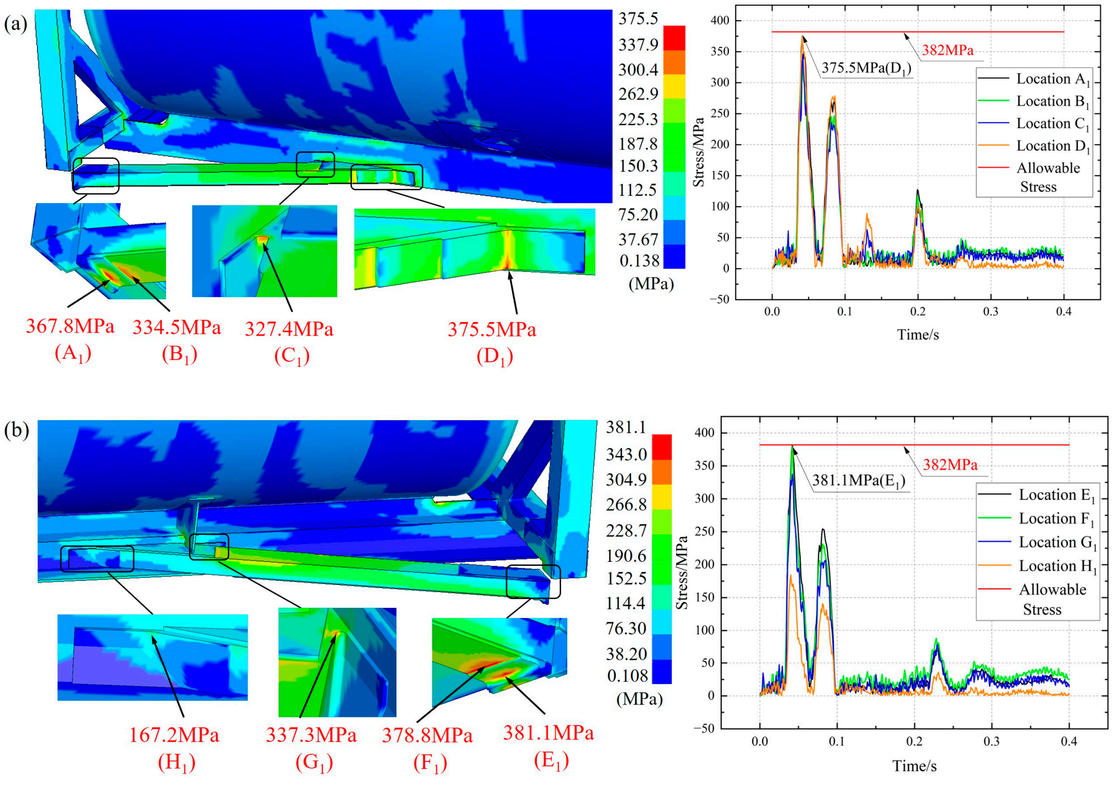

Figure 5. The stress distribution of the frame c and the variation in stress over time: (**a**) only the rear end was impacted; (**b**) only the front end was impacted.

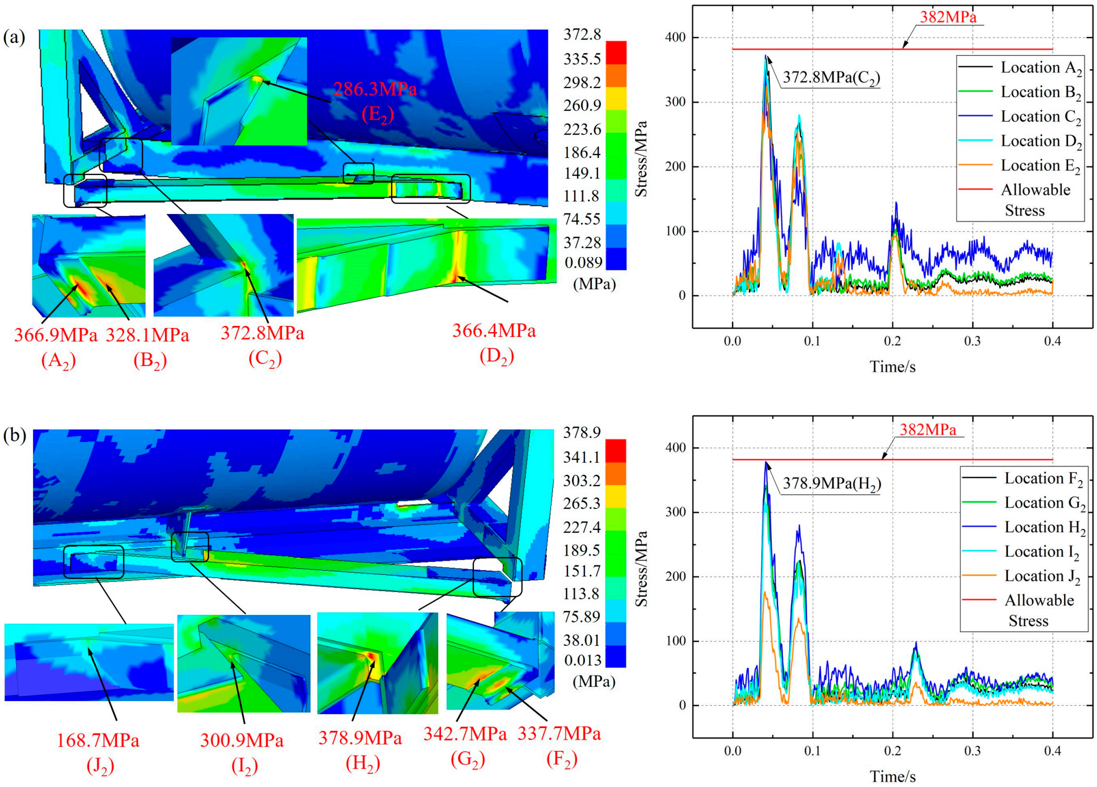

Figure 6. The stress distribution of the frame d and the variation in stress over time: (**a**) only the rear end was impacted; (**b**) only the front end was impacted.

3.2. Frame Deformation Analysis

The change in the diagonal length difference between the top, side, and impacted end of the tank after the impact test should be less than the corresponding allowable values, according to ISO 668: 2020 [27]. Figure 7 shows the measurement points of the diagonal length and the allowable values of diagonal length difference. Due to the symmetry of the finite element model about the central longitudinal section, the values of ΔK_{1a} and ΔK_2 are basically zero, so only the changes in ΔK_{1b} are analyzed.

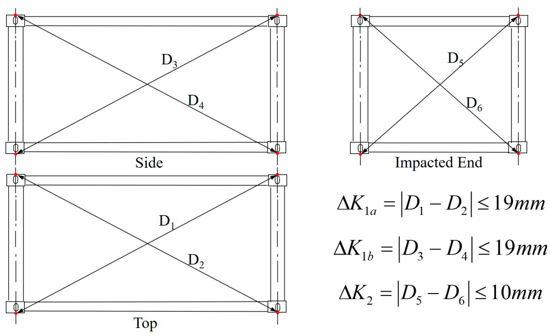

Figure 7. The measurement points of the diagonal length and the allowable values of diagonal length difference.

Figure 8 shows the variation of the ΔK_{1b} over time when only the rear or front end was impacted. It is seen that throughout the simulation process, the diagonal length differences of all the frames are less than the allowable values, meeting the requirements of the specification. In addition, it is found that the diagonal length differences of the three improved frames are less than that of the traditional frame due to the increase in longitudinal stiffness between the bottom corner fittings.

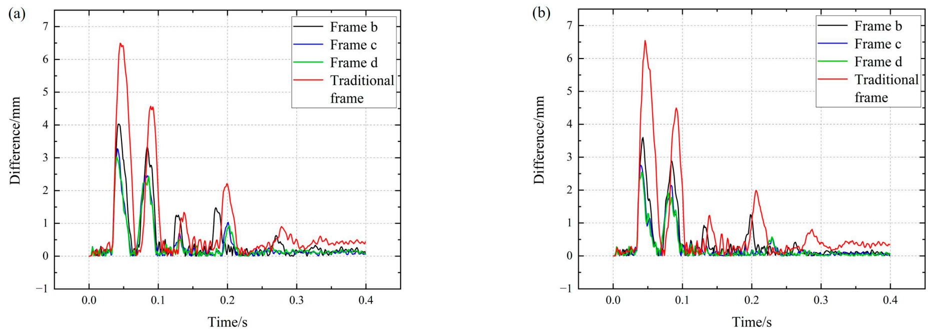

Figure 8. The variation of ΔK_{1b} over time: (**a**) only the rear end was impacted; (**b**) only the front end was impacted.

3.3. Effects on FRP Support Rings and Inner Vessels

The difference in the frames directly results in a different impact force F, which in turn affects the shaking of the LNG inside the tank container, causing the change in the impact force F_2 of the LNG on the impact side head of the inner vessel, as shown in Figure 9. F_2 greatly affects the stress distribution in the FRP support rings and the impact side heads. Figures 10 and 11 show the variation of maximum stress over time for the FRP support rings and impact side heads, respectively. It is evident that although the maximum values are different, they are still less than the respective allowable stresses, meeting the strength requirement.

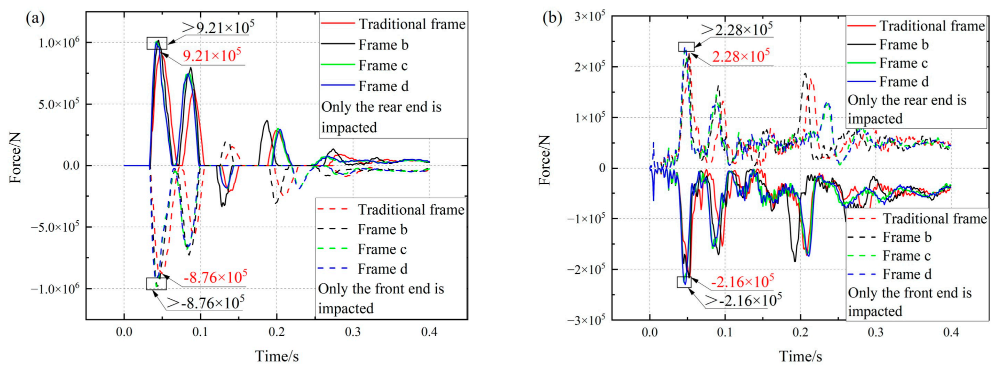

Figure 9. The variation of the impact force over time: (**a**) the impact force F, (**b**) the impact force F_2.

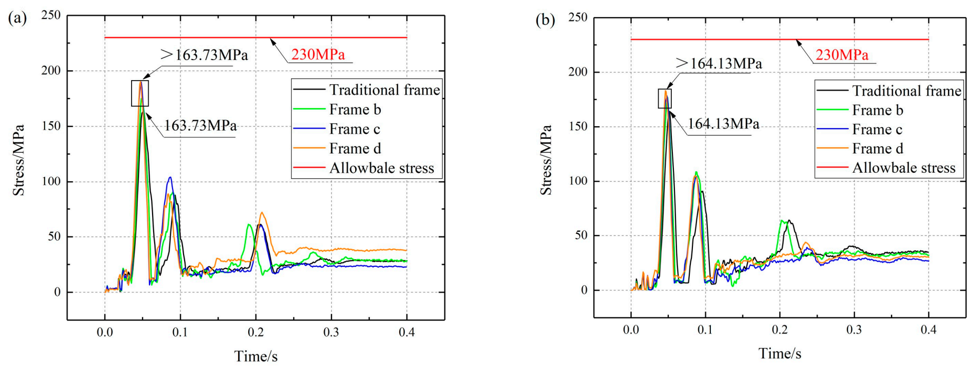

Figure 10. The variation of maximum stress over time for the FRP support rings: (**a**) only the rear end was impacted; (**b**) only the front end was impacted.

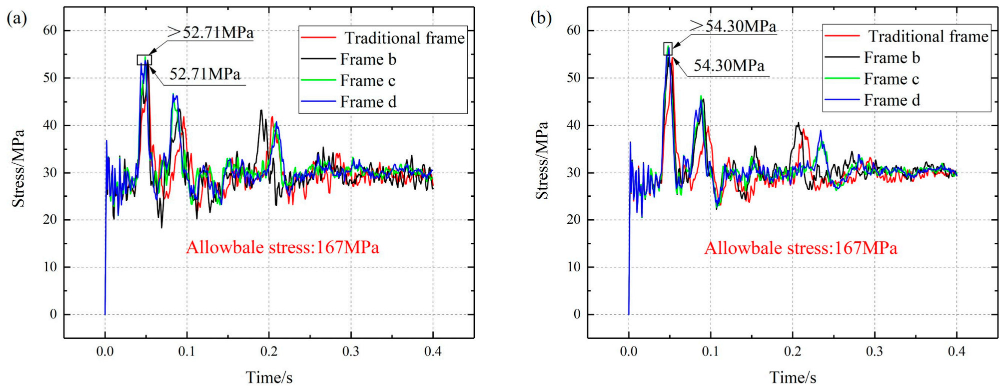

Figure 11. The variation of maximum stress over time for the impact side heads: (**a**) only the rear end was impacted; (**b**) only the front end was impacted.

3.4. Effects on Outer Vessels

Figure 12 shows the schematic diagram of the middle section of the outer vessel and the cross section of the frame connected to it, with A_3, B_3, C_3, and D_3 being the lowest locations. Figure 13 shows the change in displacement in the direction of gravity with time for these four positions over time. It is seen that in the three improved frames, the maximum displacement value occurs in frame d and is basically consistent with the maximum value of the traditional frame. The maximum value of the middle cross section of the outer vessel in the direction of gravity does not increase as a result of the change in the frame and the outer vessel remains within the elastic range, indicating that the outer vessel is still safe.

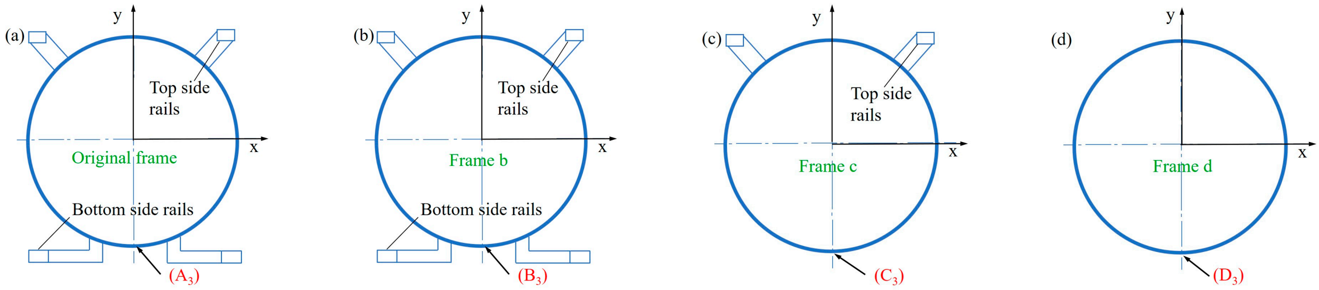

Figure 12. The schematic diagram of the middle section of the outer vessel and the cross section of the frame connected to it: (**a**) traditional frame, (**b**) frame b, (**c**) frame c, (**d**) frame d.

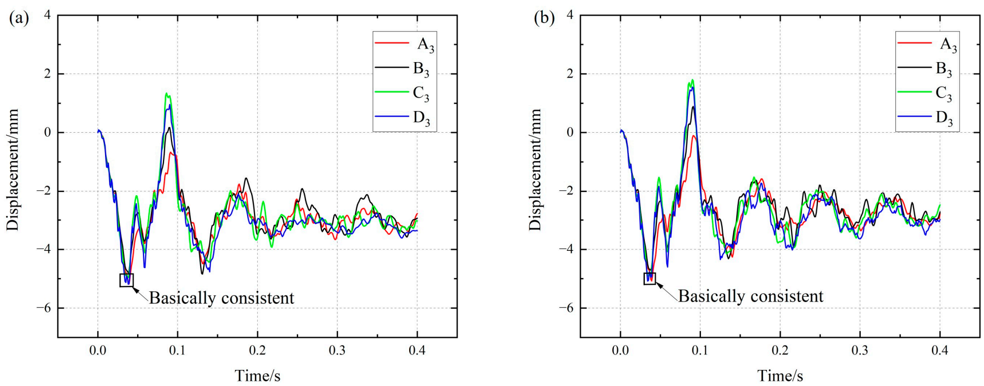

Figure 13. The displacement of four locations in the direction of gravity changes with time: (**a**) only the rear end was impacted; (**b**) only the front end was impacted.

4. Conclusions

In this paper, the stress and deformation of LNG tank container frames under impact from railway transport vehicles were analyzed, and frame structures were improved to meet strength and deformation requirements. Conclusions are obtained as follows:

1. For the problem that frames of the traditional LNG railway tank container may not pass impact strength tests, three improved frames were suggested by removing or changing side rails or bottom inclined supports.
2. All three improved frames can meet the strength and deformation requirements, i.e., the maximum Mises stress is less than the allowable stress and the diagonal length difference is less than the allowable value.
3. The improvements of the frames have little effect on the stress and deformation of the other components of the tank container, in particular, the inner vessel and outer vessel, or in other words, the stress on the tank container is still less than the corresponding allowable stress and the change in deformations will not affect the normal use of the tank container.
4. Compared to the frame of the traditional tank container, removing the side rails partially or completely reduces the weight of the frame by 17.99% and 38.34%, respectively, greatly reducing manufacturing and transportation costs.

This paper has achieved some innovative results and has some application value, but there are still some problems that need further research. For example, in the evaluation of stress and deformation, dynamic factors were not considered to assess the long-term performance and durability of the modified frame structures under repeated impact during transportation.

Author Contributions: Conceptualization, Z.W. (Zhiqiang Wang), C.Q. and Z.W. (Zhiwei Wu); data curation, Z.W. (Zhiqiang Wang); formal analysis, Z.W. (Zhiqiang Wang); investigation, Z.W. (Zhiqiang Wang), C.Q. and Z.W. (Zhiwei Wu); methodology, Z.W. (Zhiqiang Wang), C.Q. and Z.W. (Zhiwei Wu); project administration, Z.W. (Zhiwei Wu); resources, C.Q. and Z.W. (Zhiwei Wu); supervision, C.Q.; validation, Z.W. (Zhiqiang Wang), C.Q. and Z.W. (Zhiwei Wu); visualization, Z.W. (Zhiqiang Wang); writing—original draft, Z.W. (Zhiqiang Wang); writing—review and editing, C.Q. and Z.W. (Zhiwei Wu). All authors have read and agreed to the published version of the manuscript.

Funding: This research received no external funding.

Institutional Review Board Statement: Not applicable.

Informed Consent Statement: Not applicable.

Data Availability Statement: The data presented in this study are available in article.

Conflicts of Interest: The authors declare no conflict of interest.

References

1. Wang, B.; Luo, R.; Chen, H.; Zheng, C.; Gao, Y.; Wang, H.; Hashmi, A.R.; Zhao, Q.; Gan, Z. Characterization and Monitoring of Vacuum Pressure of Tank Containers with Multilayer Insulation for Cryogenic Clean Fuels Storage and Transportation. *Appl. Therm. Eng.* **2021**, *187*, 116569. [CrossRef]
2. Yu, P.; Yin, Y.; Yue, Q.; Wu, S. Experimental Study of Ship Motion Effect on Pressurization and Holding Time of Tank Containers during Marine Transportation. *Sustainability* **2022**, *14*, 3595. [CrossRef]
3. Vrabel, J.; Skrucany, T.; Bartuska, L.; Koprna, J. Movement analysis of the semitrailer with the tank-container at hard braking -the case study. *IOP Conf. Ser. Mater. Sci. Eng.* **2019**, *710*, 012025. [CrossRef]
4. Kim, T.-W.; Suh, Y.-S.; Jang, K.-B.; Chun, M.-S.; Lee, K.-D.; Cha, K.-H. A Study and Design on Tank Container for Fuel Tank of LNG Fueled Ship. *J. Soc. Nav. Archit. Kr.* **2012**, *49*, 504–511. [CrossRef]
5. Peng, J.H. Test and Analysis of LNG Tank Container Waterway Transportation. In Proceedings of the Second International Conference on Transportation Engineering, Chengdu, China, 25–27 July 2009. [CrossRef]
6. Fomin, O.; Gerlici, J.; Lovska, A.; Kravchenko, K.; Fomina, Y.; Lack, T. Determination of the strength of the containers fittings of a flat wagon loaded with containers during shunting. *IOP Conf. Ser. Mater. Sci. Eng.* **2019**, *659*, 012056. [CrossRef]
7. Fomin, O.; Vatulia, G.; Lovska, A. Dynamic load modelling for tank containers with the frame of circle pipes and structurally improved fittings. *E3S Web Conf.* **2020**, *166*, 07001. [CrossRef]

8. Fomin, O.; Gerlici, J.; Lovskaya, A.; Gorbunov, M.; Kravchenko, K.; Prokopenko, P.; Lack, T. Dynamic loading of the tank container on a flat wagon considering fittings displacement relating to the stops. *MATEC Web Conf.* **2018**, *234*, 05002. [CrossRef]
9. Sergeichev, I.V.; Ushakov, A.E.; Safonov, A.A.; Fedulov, B.N.; Fedorenko, A.N.; Brouwer, W.D.; Timofeev, M.A.; Klenin, Y.G. Structural design and strength analysis of the tank-container with composite tank for multimodal transportations of chemically aggressive fluids and petrochemical products. In Proceedings of the 20th International Conference on Composite Materials, Copenhagen, Denmark, 19–24 July 2015.
10. Muttaqie, T.; Sasmito, C.; Iskendar; Kadir, A. Structural Strength Assessment of 20-ft LNG ISO Tank: An Investigation of Finite Element Analysis and ASME Design Guidance. *IOP Conf. Ser. Earth Environ. Sci.* **2022**, *972*, 012015. [CrossRef]
11. Liguori, A.; Formato, A.; Pellegrino, A.; Villecco, F. Study of Tank Containers for Foodstuffs. *Machines* **2021**, *9*, 44. [CrossRef]
12. Ryou, Y.-D.; Lee, J.-H.; Jo, Y.-D.; Oh, Y.-S.; Cha, K.-H. Internal Pressure Variation Analysis and Actual Holding Time Test on ISO LNG Tank Container. *J. Korea Inst. Gas* **2013**, *17*, 1–7. [CrossRef]
13. de Souza, V.A.; Kirkayak, L.; Suzuki, K.; Ando, H.; Sueoka, H. Experimental and numerical analysis of container stack dynamics using a scaled model test. *Ocean Eng.* **2012**, *39*, 24–42. [CrossRef]
14. Wang, Z.Q.; Qian, C.F. Strength analysis of LNG tank container for trains under inertial force. *J. Phys. Conf. Ser.* **2020**, *1549*, 032107. [CrossRef]
15. Wang, Z.Q.; Qian, C.F.; Li, W. Study on Impact Process of a Large LNG Tank Container for Trains. *Appl. Sci.* **2023**, *13*, 1351. [CrossRef]
16. Tiernan, S.; Fahy, M. Dynamic FEA modelling of ISO tank containers. *J. Mater. Process. Technol.* **2002**, *124*, 126–132. [CrossRef]
17. Yue, W.; Chen, X. Three-Dimensional Liquid Sloshing Numerical Analysis on a New Designed Tank Container. In Proceedings of the ASME 2019 Pressure Vessels & Piping Conference, San Antonio, TX, USA, 14–19 July 2019; p. V005T09A008. [CrossRef]
18. Kim, S. Study on the numerical simulation of bird strike for composite container of external auxiliary fuel tank for rotorcraft. *J. Korea Acad.-Ind. Coop Soc.* **2017**, *18*, 709–713. [CrossRef]
19. Cao, J.; Han, M.; Qi, J.Y. The Study on Medium Filling Scheme of LNG Tank Container Impact Testing Based on ANSYS. *Adv. Mater. Res.* **2014**, *912–914*, 869–872. [CrossRef]
20. Lee, D.-Y.; Jo, J.-S.; Nyongesa, A.J.; Lee, W.-J. Fatigue Analysis of a 40 ft LNG ISO Tank Container. *Materials* **2023**, *16*, 428. [CrossRef] [PubMed]
21. Ashok, D.; Bahubalendruni, M.V.A.R.; Mhaskar, A.; Choudhary, V.; Balamurali, G.; Turaka, S. Experimental and numerical investigation on 2.5-dimensional nature-inspired infill structures under out-plane quasi-static loading. *Proc IMechE Part E J. Process Mech. Eng.* **2023**. [CrossRef]
22. Song, T.T. Research on Q450NQR1 High Strength Sheet Metal forming Springback and Application of Shallow Drawing. Master's Thesis, Shandong University, Jinan, China, 2011.
23. Pan, J.H.; Chen, Z.; Hong, Z.Y. A novel method to estimate the fracture toughness of pressure vessel ferritic steels in the ductile to brittle transition region using finite element analysis and Master Curve method. *Int. J. Press. Vessel. Pip.* **2019**, *176*, 103949. [CrossRef]
24. Han, Y. Study on Technique of Cold Stretched Austenitic Stainless-Steel Pressure Vessle and Its Performance Evaluation in Typical Media Environment. Ph.D. Thesis, Hefei University of Technology, Hefei, China, 2012.
25. Mi, L. Research on Numerical Simulation of Impact Test on Railway Vehicles. Master's Thesis, Beijing Jiaotong University, Beijing, China, 2014.
26. *TB/T 1335-1996*; Strength Design and Test Certification Specification for Railway Vehicle. China Railway Publishing House: Beijing, China, 1996.
27. *ISO 668:2020*; Series 1: Freight Containers—Classification, Dimensions and Ratings. International Organization for Standardization: Geneva, Switzerland, 2020.